EUROPEAN FUSION DEVELOPMENT AGREEMENT

EFDA–JET–CP(04)07-44

R. Sartori, P. Lomas, G. Saibene, P.R. Thomas, O. Sauter, A.Loarte, B. Alper, Y Andrew, P. Belo, T. Bolzonella, I. Coffey, C. Giroud, K. Guenther, D. Howell, L.C. Ingesson, M. Kempenaars, H.R. Koslowski, A. Korotkov, H. Leggate, E. de la Luna, G. Maddison, D.C. McDonald, A. Meigs, P. Monier Garbet, V. Parail, R. Pasqualotto, C.P. Perez, F.G. Rimini, J. Stober, K. Thomsen and JET EFDA Contributors

Scaling Study of Elmy H-Mode Global and Pedestal Confinement at High Triangularity in JET

Scaling Study of Elmy H-Mode Global and Pedestal Confinement at High Triangularity in JET

R. Sartori[1], P. Lomas[2], G. Saibene[1], P.R. Thomas[3], O. Sauter[4], A.Loarte[1], B. Alper[2], Y. Andrew[2], P. Belo[5], T. Bolzonella[6], I. Coffey[7], C. Giroud[2], K. Guenther[2], D. Howell[2], L.C. Ingesson[1], M. Kempenaars[8], H.R. Koslowski[9], A. Korotkov[2], H. Leggate[2], E. de la Luna[10], G. Maddison[2], D.C. McDonald[2], A. Meigs[2], P. Monier Garbet[3], V. Parail[4], R. Pasqualotto[11], C.P. Perez[8], F.G. Rimini[3], J. Stober[12], K. Thomsen[1] and JET EFDA Contributors*

[1]EFDA Close Support Unit (Garching), Germany
[2]Euratom/UKAEA Association, Abingdon, UK
[3]Association Euratom-CEA, Cadarache, France
[4]Association Euratom-CRPP-EPFL, Lausanne , Switzerland
[5]Associacao EURATOM/IST, Lisbon, Portugal
[6]Consorzio RFX Associazione ENEA-Euratom per la Fusione, Padova, Italy
[7]Queen's University, Belfast, UK
[8]FOM Institut voor plasmafysica "Rijnhuizen", Nieuwegein, The Netherlands
[9]Euratom Association, Trilateral Euregio Cluster, Julich, Germany
[10]Asociacion Euratom-CIEMAT para Fusion, CIEMAT, Madrid, Spain,
[11]EFDA Close Support Unit – Culham, Culham, UK
[12]Association EURATOM-IPP, MPI fur Plasmaphysik, Garching, Germany
** See annex of J. Pamela et al, "Overview of JET Results ",*
(Proc.20 [th] IAEA Fusion Energy Conference, Vilamoura, Portugal (2004).

Preprint of Paper to be submitted for publication in Proceedings of the
20th IAEA Conference,
(Vilamoura, Portugal 1-6 November 2004)

ABSTRACT.

In ELMy H modes in JET, high triangularity ($\delta \cong 0.47$) is found necessary to achieve $H_{98} = 1$ at $n_e/ n_G \geq 0.85$, the ITER requirements. This paper reports on experiments in JET to study the scaling with plasma current and edge safety factor of the global and pedestal confinement at high triangularity ($\delta \geq 0.40$). It is shown that high confinement quality (H_{98}=0.9-1) at high density ($n_e/ n_G \geq 1$) is linked with access to the mixed Type I/II ELMy regime. This regime is characterized by higher pedestal pressure at high density than with Type I ELMs, and, so far, has been observed up to 3MA. The variation in behaviour in the mixed I/II regime with δ and q_{95} is described. At the ITER q_{95} of 3, the ρ^* dependence of the global confinement scaling is confirmed up to 3.5MA (where $\rho^* \cong 1.7\ \rho^*_{ITER}$, $\nu^* \cong 5.3\ \nu^*_{ITER}$ at $n_e/n_G \cong 0.8$). In the entire range of I_p and q_{95} explored (I_p from 1 to 3.5MA, q_{95} from 3 to 5), the pedestal pressure is found to scale with I_p^2 or slightly weaker, as expected from ideal ballooning stability. The ratio between the thermal stored energy (W_{th}) and pedestal energy (W_{ped}) is similar with both Type I and mixed Type I/II ELMs, such that variations in pedestal with density, plasma current and edge safety factor are reflected in the core thermal energy.

1. INTRODUCTION

The ITER Q=10 inductively driven reference scenario [1] requires high energy confinement enhancement factor at high density: H_{98}=1 at $n_e/ n_G \geq 0.85$ (where $H_{98}(y,2)$ is the enhancement factor relative to the IPB98(y,2) scaling [2] and n_G is the Greenwald density). The positive density dependence predicted by the energy confinement scaling is not observed when the density of a Type I ELMy H-mode is increased by gas fuelling. Nevertheless, increased triangularity, δ, allows higher normalised density to be achieved whilst maintaining H_{98} sufficiently high to match the ITER requirement [3,4]. The improved confinement at higher δ is due to increased H-mode pedestal pressure. Whilst the energy confinement improvement with plasma triangularity is obtained reproducibly in several tokamaks, the triangularity required for achieving the ITER combination of H_{98} and n_e/ n_G, is different [4,5].

In JET, the ITER requirements for H_{98} and n_e/n_G at q_{95}=3 have been achieved simultaneously in the Type I ELMy regime only for δ=0.47 [5], close to the ITER value. At this δ, the density can be increased further (up to $n_e/n_G \cong 1.1$) whilst maintaining good confinement ($H_{98} > 0.9$). For $n_e/ n_G \geq 0.9$, the H-mode pedestal enters the mixed Type I/II ELM regime [5]. This regime is characterised by a 2 number of unusual features compared to the standard behaviour of Type I ELMy H-modes. First, the Type I ELM frequency decreases with increasing density (rather than the usual increase) and the pedestal pressure, p_{ped}, increases due to an increase in pedestal density at roughly constant temperature, as will be discussed in section 2. In the phases between Type I ELMs, low frequency magnetic fluctuations, as well as the inter-ELM energy losses, are enhanced compared to the Type I ELMy regime. Although no D_α bursts are observed in JET in between Type I ELMs, the features observed in the inter-ELM phase of those high density H-modes are similar to those observed in ASDEX Upgrade in Type II ELMy H-modes [6]. As discussed later, the mixed Type I/II ELM regime is generally observed in JET at $\delta > 0.4$. Access to this regime seems to be a necessary

condition to achieve high density and maintain good confinement at the same time.

The main aims of the experiments reported here are: To study the scaling with plasma current and edge safety factor of the pedestal and global confinement in ELMy H-modes at high triangularity and density; To explore the operational space of mixed type I/II ELMs. Other aspects of JET studies connected with this experiments are reported elsewhere: a study of the ELM energy and particle losses of JET plasmas over a wide range of parameters, including the high triangularity H-modes described here, is reported in [7]. The behaviour of impurity seeded high δ ELMy H-mode is analysed in [8].

2. DESCRIPTION OF THE EXPERIMENT

The good confinement at high density reported in [5] was obtained in a plasma configuration with $\delta \cong 0.47$, called "ITER-like" configuration, at $I_p = 2.5$MA and toroidal field $B_t = 2.7$T, with $q_{95} \cong 3$. With the present JET divertor, operation with $\delta \cong 0.47$ is limited to 2.5MA. In order to extend the achievable range of plasma current at high triangularity, a configuration with reduced triangularity, $\delta \sim 0.42$, and somewhat larger q_{95} for the same I_p/B_T ($q_{95}=3.6$ at 2.5MA/2.7T) was designed for operation up to 3.5MA. Compared with the ITER- like configuration, the new configuration, HT3, has larger minor radius ($a \cong 0.93$-HT3, $a \cong 0.89$-ITER-like), similar elongation ($\kappa \cong 1.72$), lower X-point position and lower relative VDE force.

Density scans with deuterium gas fuelling and combined NBI and ICRF heating were performed in the HT3 configuration with plasma current I_p from 1 to 2.5 MA at $q_{95} \sim 3.6$, with I_p from 2.5 to 3.5 MA at $q_{95} \sim 3.0$, and with $I_p = 2.5$MA at $q_{95} \sim 4.6$. The range of dimensionless parameters spanned in this experiment is shown in Figure 1. The figure summarizes the normalized Larmor radius $\rho*$ and collisionality $\nu*$ relative to the ITER values that were obtained in the I_p and q_{95} scans. The closest match to the ITER required combination of $\rho*$ and $\nu*$ for $n_e/n_G \geq 0.8$ was obtained, as expected, at 3.5MA/3.2T ($q_{95}=3$): $\rho* \cong 1.7 \rho*$ITER, $\nu* \cong 5.3\ \nu*$ITER at $n_e/n_G \cong 0.8$, $n_e \cong 11 \times 10^{19}$ m^{-3}, $P_{NB} \cong 22$MW.

In all cases, additional heating was a combination ofNBI and 2 to 3.5 MW of ICRH power (H minority central resonance with dipole phasing). The ICRH power (providing $\leq 20\%$ of the total additional heating power) is limited by difficulties in coupling with Type I ELMs. The overall decrease in βN at lower $\rho*$, shown in Fig 1, also reflects the fact that there is not sufficient installed power: the required additional heating power, P_{IN}, for an Hmode at given n_e/n_G increases approximately as the product $I_p * B_t$, since $P_{L\text{-}H} \propto n_e B_t$ and $n_e - I_p$.

The analysis of the global and pedestal confinement is restricted to plasmas with steady density profiles. Typically, these high density ELMy H-modes have rather flat density profiles, with peaking factor (defined here as the ratio of the line averaged density from a central and an edge cord of the interferometer which determines the pedestal density) of $\cong 1.2$. Continuous peaking of the density profile was observed below a minimum input power that depends on I_p and B_T and is avoided with central ICRH heating. If not controlled, this continuous peaking leads to impurity accumulation and eventual disruption. The minimum input power requirement for those experiments was not limited by the L-H transition, but by the minimum P_{IN} required to avoid the continuous density peaking.

The requirements for the minimum length of the additional heating phase can be demanding at high I_p: not only does it take 6-8τ_E in those high δ ELMy H-modes for the density to reach a steady value, but a further $\geq 6\tau_E$ with steady plasma parameters is preferred to obtain high quality confinement data. In addition, the external fuelling required to reach a given n_e/n_G increases with I_p (and with P_{IN}, for fixed I_p). This conflicts with the re-ionisation limit on pressure in the NBI ducts which determines the achievable pulse length.

A (3,2) NTM was sometimes triggered by a sawtooth crash in the initial phase of the additionally heated plasma, when density, input power and magnetic configuration are ramping up to their final value and the plasma makes the L-H transition. The low q_{95}~3 domain was more prone to those NTMs. However, a NTM avoidance scenario was developed, reducing substantially the occurrence of large (3,2) modes (to less than 10% at q_{95}=3), which can degrade confinement by 10-20%[8]. In the NTM avoidance scenario this lower density phase has high power and also higher q_{95} and lower δ than the steady ELMy H-mode: the final values of q_{95} and δ are reached only at high density. Discharges with (3,2) NTMs have been excluded from the confinement analysis.

3. GLOBAL CONFINEMENT RESULTS

3.1. THE MIXED TYPE I/II ELMY REGIME AT HIGH DENSITY

The mixed Type I/II ELMy regime was found at high density also with the new plasma configuration HT3 at the reduced $\delta \cong 0.42$. The characteristic signatures [see also 5,6] of the mixed Type I/II ELMy regime in global and pedestal parameters are most clearly visible in the gas scan at 2.5MA/ 2.7T, $q_{95} \cong 3.6$. The first characteristic is the “anomalous” behaviour of the Type I ELM frequency, fELM. At lower triangularity f_{ELM} increases monotonically with density. In the low density range ($n_e/n_G \leq 0.9$), f_{ELM} increases with density also at high δ. However, as the density is increased, a density range exists where f_{ELM} decreases with density. When the density is increased further, f_{ELM} increases again and phases with Type III ELMs are observed. The transition to a steady Type III ELMs regime, with reduced confinement, is observed at the highest fuelling rate. In the density range where f_{ELM} decreases, H98y=1 was obtained with n_e/n_{GR} from 1 to 1.1, corresponding to an absolute density $\geq 9\ 10^{19} m^{-3}$ (see Fig.2).

Figure 3 shows that this improved confinement quality correlates with increased pedestal pressure relative to the highest density Type I data. The figure shows the evolution of the pedestal parameters n_e, T_i (red triangle) and T_e (red circles) for the same set of discharges of Fig.2. The pedestal T_i is measured with Charge Exchange Spectroscopy (at a fixed position, R=3.76-3.78m), T_e with ECE (at the pedestal top) and n_e is the pedestal line averaged density from the FIR interferometer (at R=3.75m). At low density, in the Type I ELMy regime, the pedestal pressure, p_{ped}, decreases with density (Fig.3), as is typical for JET Type I ELMy H-modes [3]. In other words, the pressure falls below the curve pped=constant shown. At constant P_{IN}, this corresponds to an initial limited decrease of the total thermal stored energy, W_{th}. At higher density, the increase in p_{ped} is due to an increase of n_e at almost constant T_i (W_{th} increases). As shown in Fig.4, in this phase the pedestal energy recovers the same value (or higher) than at low density. When the fuelling is increased further, both ne and

T_i (W_{th}) decrease. When this happens, the inter-ELM, Type II-like behaviour (see section 4) is still observed but with reduced p_{ped} and global confinement. Phases with Type III ELMs also start to appear. At the highest fuelling rates the H-mode has only steady Type III ELMs.

The Type I/II ELM regime at high density was found with q_{95} = 3.6 and also with q_{95} = 3, at 2.5 and 3MA. At 3.5MA the gas scan was limited to lower density and the higher density range is yet to be explored. At the highest q_{95} explored (q_{95} > 4.5) the H-modes had Type I ELMs over the entire density range, up to the transition to Type III ELMs at the highest density (see discussion in paragraph 3.3)

.

3.2. PLASMA CURRENT SCAN AT Q_{95} = 3

Figure 5 shows the confinement enhancement factor for the density scans at q_{95} = 3, with I_p/B_t of 2.5MA/2.25T, 3MA/2.7T and 3.5MA/3.2T. Although the relative improvement of the mixed Type I/II ELM regime over the Type I ELM is observed also at this lower q_{95}, H_{98} is generally lower than at q_{95}~3.6 (H_{98} = 0.9 to 0.95 compared to H_{98} = 1 at q_{95} = 3.6: see the comparison with the grey triangles in Fig.5).

Figure 6 shows the time evolution of some global plasma parameter for three high density discharges at 2.5, 3 and 3.5MA. The discharges at 2.5 and 3MA are in the mixed Type I/II regime, while the H-mode at 3.5MA, at lower normalised density, has Type I ELMs.

The discharges at 2.5 and 3MA have similar β_N (2 and 1.9) and similar normalised density of 0.99 n_G while β_N=1.6 at 3.5MA. The increase in absolute density and in stored energy with I_p is seen clearly. Fig.5 might suggest some decrease in H factor from 2.5 to 3 MA, which might be due to two factors. First, some of the 3MA plasmas have a (4,3) NTM, in particular in the low density range, while the 2.5MA plasmas have no (4,3) NTM. The (4,3) mode can produce a degradation of the confinement up to 10%[9], and explains why the confinement at the lowest density is higher at 2.5MA than at 3 MA. Secondly, the confinement data does not show the positive density dependence of the scaling law, and therefore the H factor will tend to decrease with I_p simply because higher absolute densities are obtained. Furthermore, in the gas scan at 3MA the input power had a larger variation (towards lower power) than at 2.5MA. Taking into account the above considerations, the H factor is effectively constant for the three levels of plasma current explored both in the Type I and mixed Type I/II ELMy regimes, confirming the I_p dependence of the H_{98} scaling. In the 3MA H-modes the increase in fuelling was limited by the maximum fuelling allowed by the NB system (duct pressure limit), hence lower normalised density was achieved 3MA compared to 2.5MA.The increase in the pedestal density and temperature with plasma current, is shown in Fig.7 and discussed also in paragraph 3.4.

3.3. Q_{95} SCAN

At I_p = 2.5MA a gas scan was carried out for three values of q_{95}: 3, 3.6 and 4.6. The n_e-T_i pedestal diagram of the 2.5MA plasmas at q_{95} = 3 (blue diamonds) are compared in Fig.7 with the data at q_{95} = 3.6 (grey triangles) and q_{95} = 4.6 (grey squares). The comparison with the q_{95} = 3.6 data shows

that at q_{95} = 3 the pedestal density in the mixed Type I/II ELMy regime is similar, but pedestal temperature is lower. The reduced pped at q_{95} = 3 is consistent with the lower H factor in the global confinement analysis. Similarly, at lower density in the Type I domain, the q_{95}=3 data shows lower H factor and lower pedestal temperature at the same density compared to q_{95}=3.6. No general trend of decreasing global confinement with decreasing q_{95} is observed in JET data [10].

At higher q_{95}~4.6, both pedestal and global confinement are also lower than at q_{95}~3.6 (see Fig.5 and 7). The largest difference at q_{95}=4.6 is that the achievable density was limited to low value (0.85 n_G) by the transition to Type III ELMs. This prevented access to the mixed Type I/II regime and hence to the improved confinement associated with it. The comparison with the q_{95}=3.6 data shows that the critical density for the transition to Type III ELMs is consistent with the $n_{crit} \propto B_t / q_{95}^{1.25}$ scaling found for JET data [11]. Still, at the lower q_{95} of 3.6, it was possible to achieve higher density in the Type I/II ELM regime than the density before the Type III transition. It is possible that the lower power available for this experiment at q_{95}=4.6 was insufficient to prevent the transition to Type III ELMs at high density [12]. However, experiments at lower I_p and q_{95}~5 [5], where the power relative to Hmode threshold was higher, were also limited at high density by a transition to Type III ELMs. This suggests that the mixed Type I/II ELM regime might be, in JET, intrinsically difficult to achieve at high q_{95}, possibly due to the relative changes of the Type III and Type I/II ELM boundaries [6].

The comparison, at 2.5MA/2.7T, of the results achieved with the HT3 configuration and the results with the higher triangularity ITER-like configuration shows that, in the mixed Type I/II regime (n_e>0.9n_G), overall the ITER-like at q_{95}=3 as similar H factor as the HT3 at the same q_{95}. In the Type I ELMy regime, instead, the confinement at the same I_p/B_t is similar (ITER-like at q_{95}=3 and HT3 at 6 q_{95}=3.6). This result might indicate some trade off between δ and q_{95} for the achievement of high confinement at high normalised density.

3.4 Relation between pedestal and core confinement

Fig.8 shows that the ratio between pedestal and thermal stored energy, W_{ped}/W_{th}, is 0.4 to 0.5 for all our experiments, from 1 to 3.5MA. W_{ped} is calculated assuming $n_{ped}=n_{iped}=n_{eped}$ and $T_{ped}=T_{iped}=T_{eped}$, i.e, $Wped=3n_{eped}T_{iped}V_{plasma}$. The ratio W_{ped}/W_{th} is similar for both Type I and mixed Type I/II ELMs, confirming that the good global confinement with Type I/II ELMs at high density results from the high pedestal pressure, characteristic of this regime. The pedestal pressure is found to scale approximately as $I_p^{\,2}$ or slightly weaker (see Fig.9) as found also in [6] and as expected from ideal ballooning stability.

The data of core and pedestal confinement were compared with two “two term” scaling proposed by the ITPA confinement and pedestal working groups [13]. The two models behind the scaling are assuming two different energy loss mechanisms from the pedestal: the first scaling (1), assumes the transport in the steep edge gradient region to be dominated by thermal conduction, while the second (2) assumes ELM losses to be dominant and the pedestal pressure gradient to be determined by MHD limit (ballooning or peeling modes).

The MHD limit scaling fits marginally better the experimental pedestal energy with $W_{ped} \cong 1.5 Wped(2)$ and standard deviation of 0.22, compared to 0.27 for thermal conduction based scaling. The fitting of W_{core} gives similar standard deviation for both scaling. Since the two scaling fit the data with similar accuracy, the analysis does not allow to identify which model better describe this set of data.

The fitting of W_{ped} and W_{core} for the MHD based model is shown in Fig.10 and 11. The vertical spread of the pedestal data is due to the density dependence of the pedestal pressure that is illustrated in Fig.4 and which is not accounted for in either scaling. It has also to be noted that for this set of data, power and Ip are correlated variables (W_{ped} (1)$\propto I_p^{1.58} P^{0.42} B^{0.06}$), since P_{IN} was increased proportionally to $I_p B_t$ and, although for fixed I_p/B_t there seems to be some increase in the pedestal pressure with power, the variation of power is too limited to detect any trend.

4. ELM ENERGY LOSSES

Figure 12 shows that the transition from the Type I to the mixed Type I/II ELMy regime is characterized by a reduction of the normalised power loss by the ELMs, $f_{ELM}\Delta W/Psep$ (where ΔW is the prompt energy loss per ELM averaged over, typically, 8-10 ELMs), in agreement with previous results [5]. Although the scatter of the data is large, there seem to be a correlation between $f_{ELM}\Delta W/P_{sep}$ of mixed Type I/II ELMs and their pedestal pressure, with higher p_{ped} for decreasing ELM energy losses. In Fig.13, the MHD fluctuation spectra of a q_{95}=3 Type I ELMy plasma, and of two plasma at the same q_{95} with mixed Type I/II ELMs are compared.

Although the characteristic enhancement of the MHD fluctuations at lower frequencies is observed also at q_{95}=3, it is less pronounced than at higher q_{95}=3.6, as shown in Fig.14. Both MHD and ELM loss measurements confirm that the mixed Type I/II ELMy regime is achieved also at q_{95}=3, but with weaker signature in the MHD fluctuation change. The normalised Type I ELM prompt energy losses decrease with increasing pedestal collisionality [5], but the points at high q_{95}(q95>4) are below the general trend of the data. It has been shown in [6] that increasing q_{95} leads to smaller ELMs for the same plasma collisionality, mainly through a reduction of the conductive losses ($\Delta T_e/T_e$), and that at high delta this reduction is larger compared to lower triangularity, leading to small Type I ELMs, even at low collisionality.

CONCLUSIONS

A study of the behaviour of pedestal and global confinement of high triangularity ($\delta \geq 0.4$) ELMy Hmodes was carried out in JET. Density scans were carried out for a wide range of plasma parameters, with I_p from 1 to 3.5MA and q_{95} from 3 to 4.6. The closest match of the ITER parameters in terms of the combination of $\rho*$, $\nu*$ and n_e/n_G was obtained, as expected, in discharges at 3.5MA/3.2T (at q_{95}=3), with $\rho* \cong 1.7\ \rho*$ ITER, $\nu* \cong 5.3\ \nu*$ITER at $n_e/n_G \cong 0.8$ and with $n_e \cong 11 \times 10^{19}$ m^{-3}.

The possibility to obtain high H-factor ($H_{98} \cong 0.9$ to 1) for densities at, or in excess of, the Greenwald limit was found to be linked to the plasma access to the mixed Type I/II regime. For any

I_p/B_t combination, when the density is increased by external fuelling the plasma shows the characteristic behaviour of Type I ELMs: the pedestal pressure decreases with increasing pedestal density, the energy confinement enhancement factor decreases with density, the ELM frequency f_{ELM} increases. At high triangularity and high density (typically $n_e/n_G \geq 0.85$-0.9) the plasma might access the mixed Type I/II regime, characterised by an increase of the pedestal density at approximately constant temperature, by a decrease of the Type I ELM frequency and of the power loss by the ELMs, and by an enhancement of the inter-ELM magnetic fluctuations in the low frequency range. When this happens good global confinement at high density is observed with H_{98} up to 1 for density $\geq n_G$. Although this regime was observed at both at q_{95}=3 and 3.6 and for I_p up to 3MA (at 3.5MA the high density range was not explored), it was not possible to access the regime at the highest q_{95} (q_{95}.>4.6, I_p=2 and 2.5MA and results reported in [5]). In those cases, both pedestal parameters and f_{ELM} were typical of Type I ELMs, up to the transition to Type III ELMs at high density, and the H factor obtained at high density was lower. The reason of this behaviour at high q_{95} is not clear and will be explored in future experiments. It might be related with the changes of the Type III boundaries with q_{95} and B_t.

The ratio between pedestal and thermal stored energy W_{ped}/W_{th} does not vary from Type I to mixed Type I/II ELMs, showing that the improved confinement at high density with Type I/II ELMs is due to the increased pedestal pressure and not to changes in the core profiles. W_{ped}/W_{th} was between 0.4 to 0.5 in all the range of I_p and q_{95} explored.

In the Ip scan at q_{95}=3, the increased pedestal temperature and density with I_p was clearly seen with both Type I and mixed Type I/II, leading to constant H factor and confirming the $\rho*$ dependence of the scaling. More generally, the pedestal pressure is found to scale as $I_p^{\,2}$ or slightly weaker in the entire range of parameters explored, with mixed Type I/II ELMs being above the scaling.

Although the mixed Type I/II regime was accessed at q_{95}=3, both pedestal and global confinement were lower than at q_{95}=3.6, which can be most clearly seen by the comparison at I_p=2.5MA. Although the difference in confinement at high density is not large (≤10%), it is consistently seen in both pedestal (lower Tped for the same nped) and global confinement (lower H_{98}). In addition, both MHD fluctuation and ELM energy loss measurement suggest a weaker Type I/II signature at the lower q_{95} of 3. The comparison with previous data at higher δ ($\delta \cong 0.47$) and lower q_{95} also suggests some trade off between q_{95} and δ in the mixed Type I/II regime.

REFERENCES

[1]. Campbell, D.J, et al., "The Physics of the International Thermonuclear Experimental reactor FEAT", Phys Plasmas **8** (2001) 2041.

[2]. ITER Physics Basis, Nucl Fus **39** (1999) 2175

[3]. Saibene, G, et al, Nucl Fus **39** (1999)

[4]. Stober, J, at al, Plasma Phys. Cont. Fusion **42** No 5A (2000), A211

[5]. Saibene,G, et al, Plasma Phys. Cont. Fusion **44** (2002),1769

[6]. Stober, J, et al, these proceedings
[7]. Loarte, A, et al, Phys Plasmas **11** (2004) 2668.
[8]. Monier Garbet, P, et al, these proceedings
[9]. Buttery, R, these proceedings
[10]. McDonald, DC, et al, Plasma Phys. Cont. Fusion **46** (2004), A215
[11]. Chankin, A and Saibene, G, Plasma Phys. Cont. Fusion **41** (1999), 913
[12]. Sartori, R, et al, Plasma Phys. Cont. Fusion **44** No 5A (2002), 1801
[13]. Cordey, J.G. for the ITPA H-mode database Working group and the ITPA Pedestal database Working Group, Nucl Fus **42** (2003), 670

.

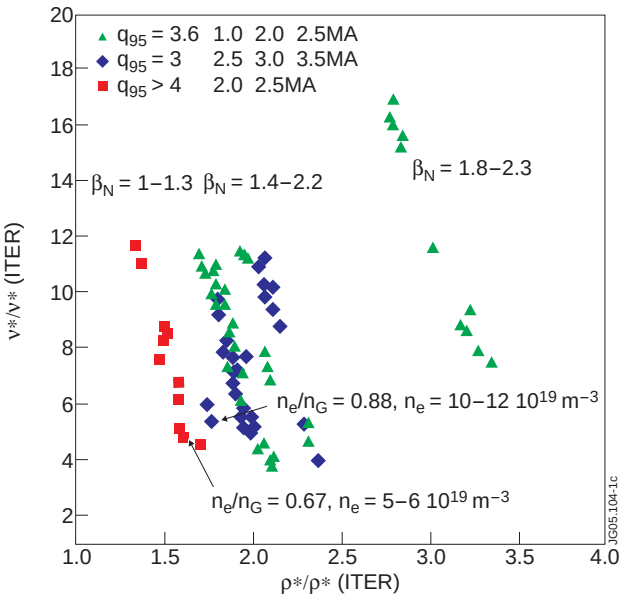

Figure 1: Dimensionless plasma parameters ρ and ν* (normalized to the ITER values for the ELMy H-mode standard scenario) for the density scans at different I_p and q_{95}.*

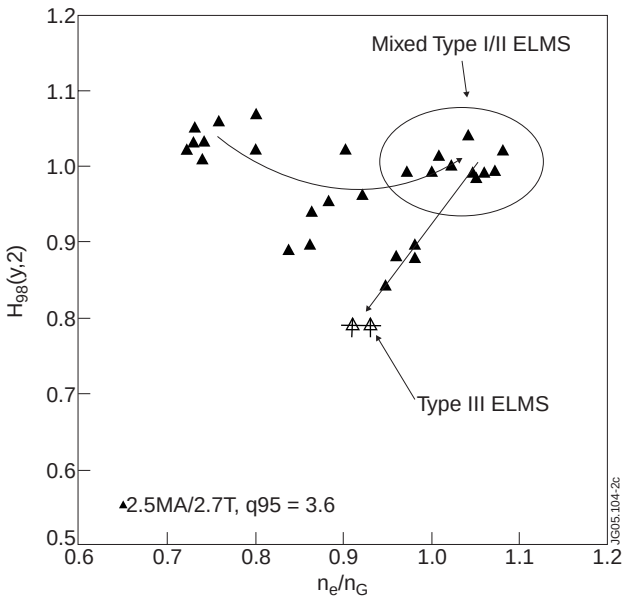

Figure 2: H_{98} versus normalised density at 0.5MA/ 2.7T(q_{95}=3.6). The arrows indicate increasing gas fuelling

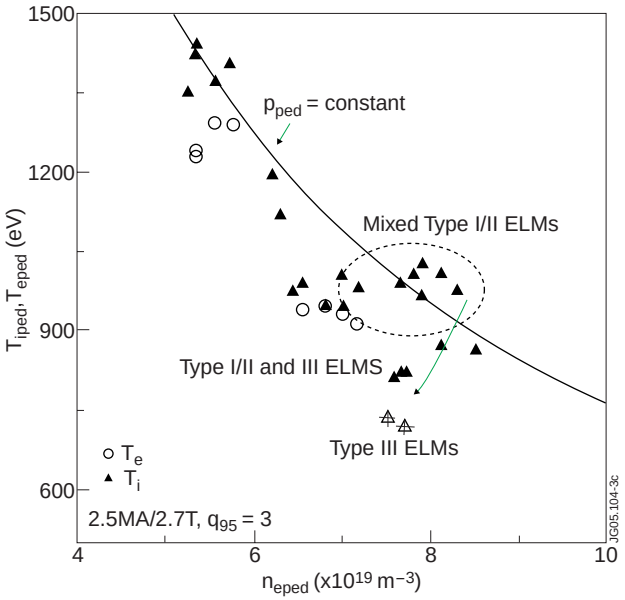

Figure 3: Pedestal temperature (T_i, T_e) vs pedestal density n for the same set of data as Fig.1e. Due to ECE cut-off, T_e data are only available at low density

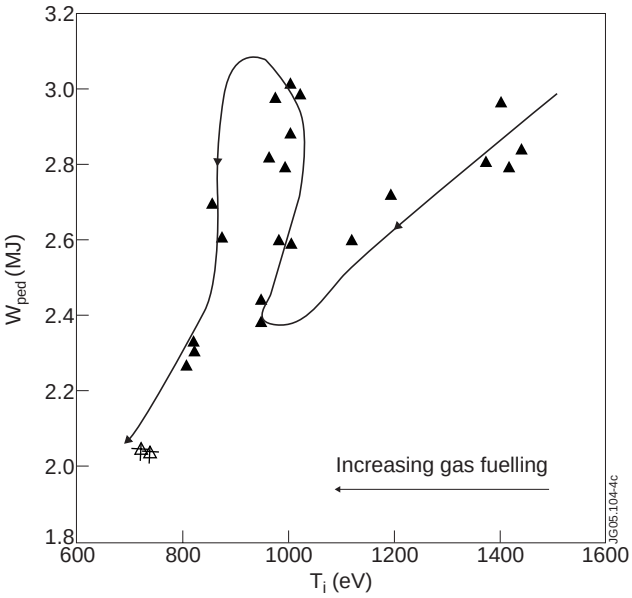

Figure 4: Pedestal energy versus pedestal temperature for the same set of data as Fig.1

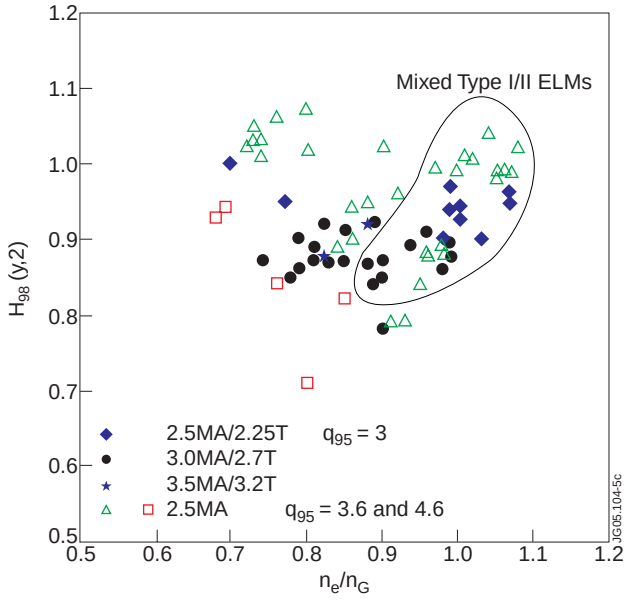

Figure 5: H factor versus normalised density for the I_p scan and q_{95} scan at lower normalised density, has Type I ELMs.

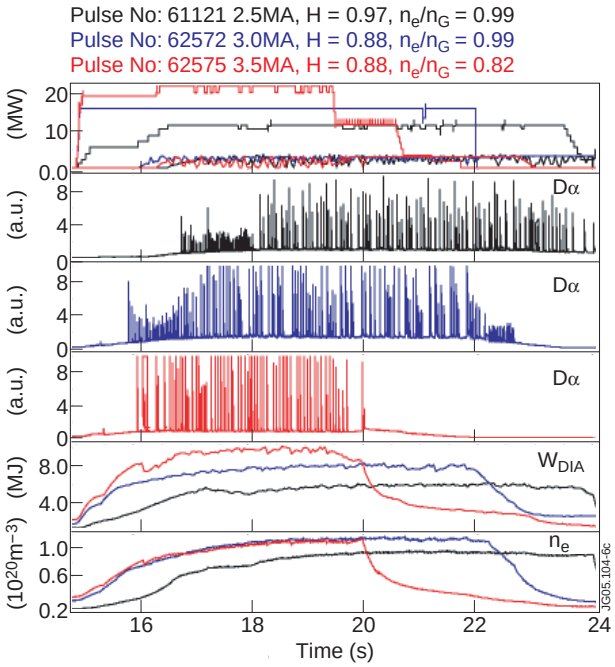

Figure 6: Time traces of NBI and ICRH input power, Dμ, diamagnetic stored energy and plasma density for three discharges at 2.5, 3.0 and 3.5MA, q_{95}=3. At 3 and 3.5MA the NB heating is prematurely terminated because the limit in the NB duct pressure is reached

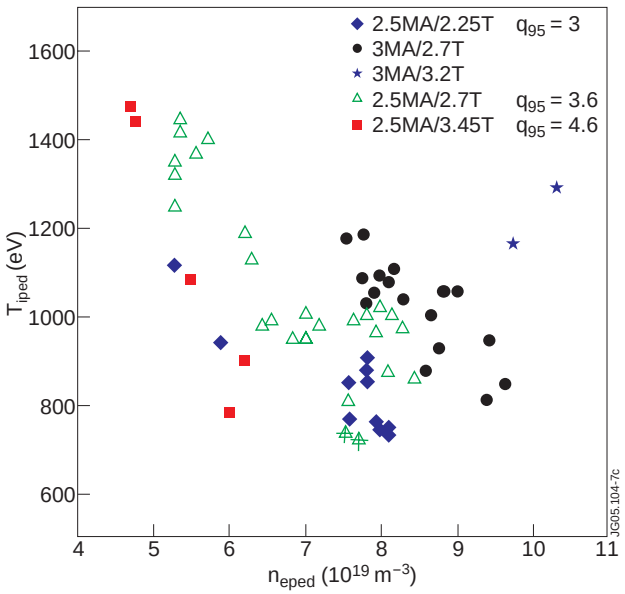

Figure 7: Pedestal n_e-T_i for the I_p scan and q_{95} scan

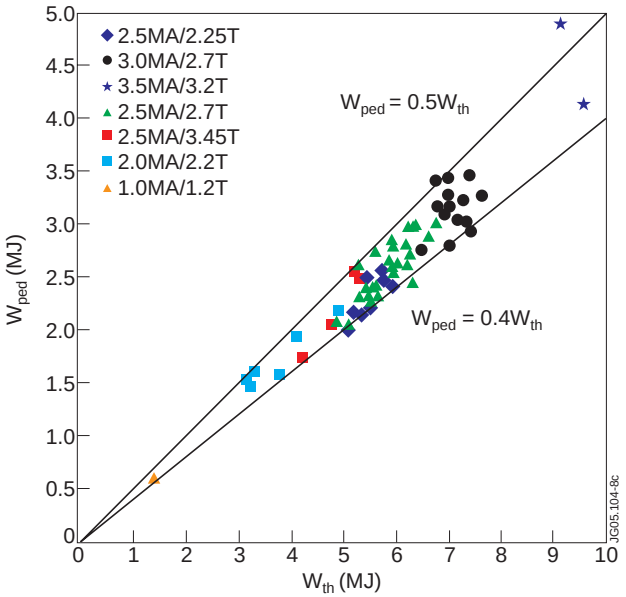

Figure 8: Pedestal versus thermal stored energy for the entire set of data

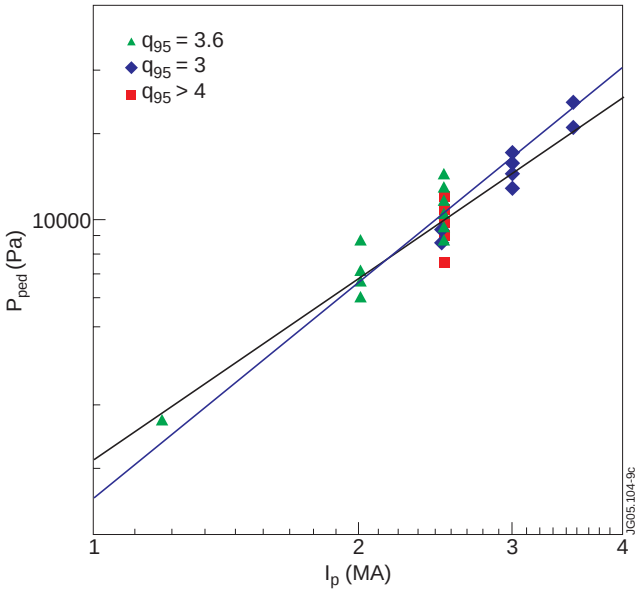

Figure 9: Pedestal pressure versus plasma current for the entire set of data

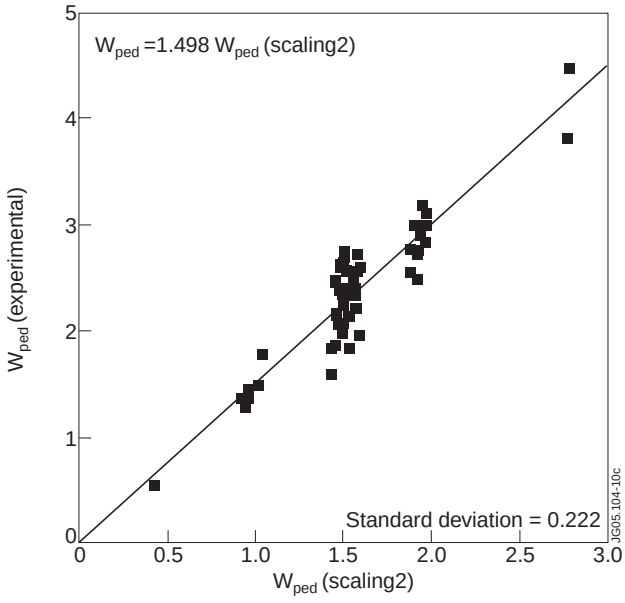

Figure 10: Scaling of the pedestal stored energy W_{ped} (2)=$RI^2\beta_{ped}$=$RI^2 6.4310^{-4}\rho^{*0.3}m^{0.2}F_q{}^{2.18}\varepsilon^{-2.67}k_\alpha$ 2.27

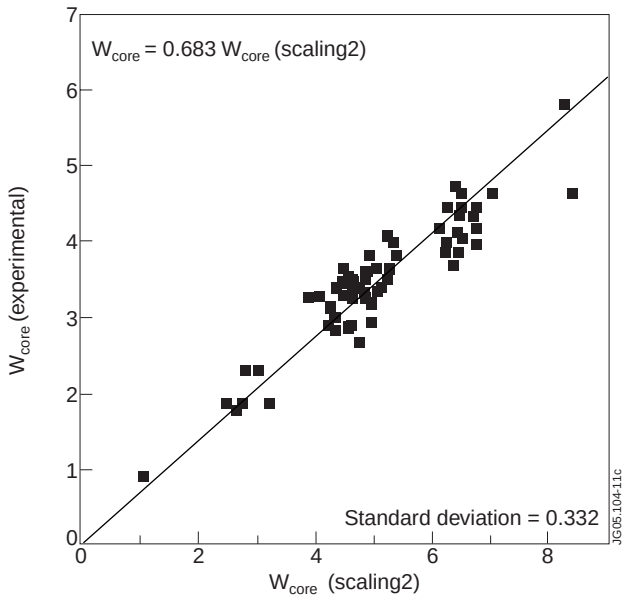

Figure 11: Scaling of the core stored energy $W_{core}(2)=0.151I^{0.68}R^{2.32}P^{0.42}n^{0.59}B^{0.13}k^{-0.34}\varepsilon^{1.96}m^{0.34}$

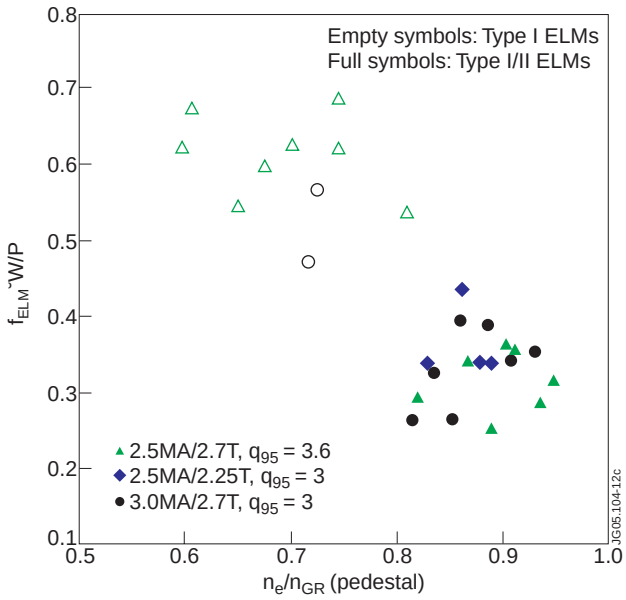

Figure 12: ELM energy losses normalized to the power to the separatrix vs normalized pedestal density for the gas scans at q_{95}*=3.6 (2.5MA, red) and* q_{95}*=3 (2.5MA, black, and 3MA,green)*

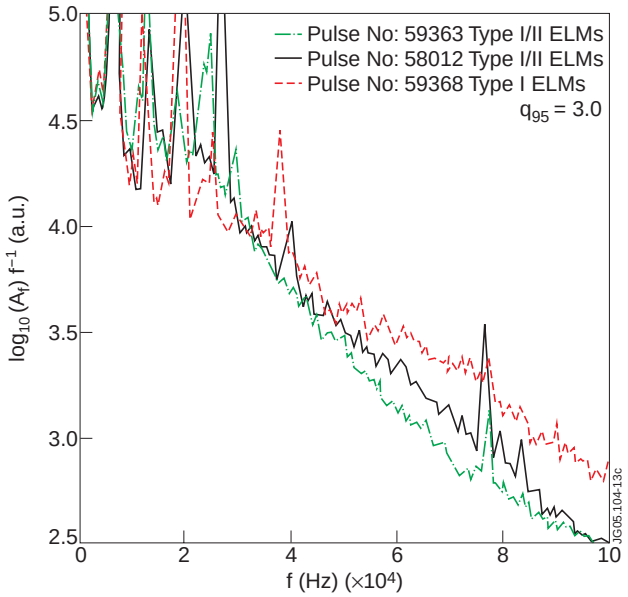

Figure 13: Spectra of the magnetic fluctuation in the inter-ELM period for Pulse No's: 59368 (red, 3MA/2.7T, Type I ELMs), 58012,(black, 2.5MA/2.25T, Type I/II ELMs) and Pulse No: 59363 (green, 3MA/2.7T, Type I/II ELMs)

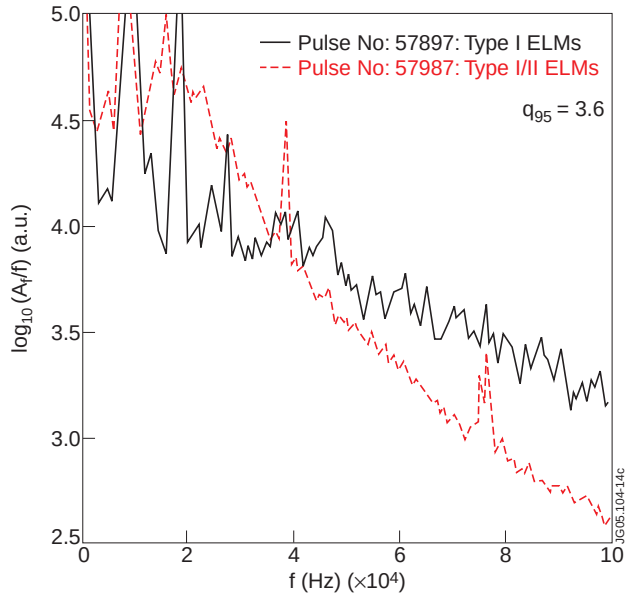

Figure 14: Spectra of the magnetic fluctuation in the inter-ELM period for Pulse No: 57987 (green) and Pulse No:57897 (blue). An enhancement of the fluctuations in the low frequency range is observed with Type I/II ELMs.